

## Color Values and Spectra of the Principal Emitters in Colored Flames

W. Meyerriecks\* and K. L. Kosanke†

\*702 Leisure Avenue, Tampa, FL 33613, USA

†PyroLabs, Inc., 1775 Blair Rd, Whitewater, CO 81527, USA

### ABSTRACT

The emission spectra of many of the more important emitters in pyrotechnic flames were collected. For this purpose solutions and suspensions of sodium, potassium, calcium, strontium, barium and copper salts were aspirated into a propane gas flame as the excitation source. Performing instrument corrections and using appropriate data reduction strategies allowed the isolation of the individual spectra. Among these are the monochlorides and monohydroxides of strontium, calcium, barium and copper. The CIE color coordinates of the principal emitters were calculated from the isolated spectra. In addition, a table of normalized band and line intensities was produced for each of the successfully isolated emitting species.

**Keywords:** flame spectra, flame color, color emitter, color coordinate, monochloride, monohydroxide, barium, calcium, copper, strontium

### Introduction

The desire to produce improved flame color has been an enduring goal of pyrotechnists. However, over the last century, much of the effort in that quest has not been guided by accurate spectral information. Two pioneers in quantifying this work were T. Shimizu<sup>[1]</sup> and B. E. Douda.<sup>[2-4]</sup> Most recently, with the introduction of relatively inexpensive computer-based spectrometers,<sup>[5]</sup> hard-data—rather than subjective impressions—are being more widely used to guide developments. However, to date, the lack of relatively complete and reliable information on the spectra and CIE color coordinates of the

individual colored flame emitters remains as an impediment.

Shimizu, in his textbook,<sup>[6]</sup> was probably the first to address the assignment of a series of the principal colored flame emitters to their position in the chromaticity diagram. Nevertheless he made essentially no attempt to determine the composite chromaticity values (color coordinates) for emitters having more than one narrow spectral line such as sodium. Instead he made a series of somewhat expressionistic intensity assignments for the respective lines, such as for potassium, and assignment of the bands of the monochlorides and monohalides of the alkaline earth metals and copper.

Several reference texts are available with tables of wavelengths and peak intensities for atomic and molecular visible-light emitters.<sup>[7-11]</sup> Unfortunately they are somewhat incomplete and even contradictory. The intended use of these tables seems to be primarily geared towards analytical chemistry—for identifying the probable emitting atom or molecule for a given line or band present in a spectrum. (An extensive table, compiled from some of these sources, and including the authors' current work, has been appended to this paper.) Further, very few of the reference texts include actual spectra for the various emitters, and when they do, instrumentation effects have not been removed. What is generally presented are the “raw readings” directly from the instrument, which often includes many different emitting species.

No reference text that the authors have seen has presented isolated spectra for the various individual colored flame emitters. Having such data would allow the investigator to more accurately determine the emitting species present in the spectra of test compositions, and thus be bet-

ter able to rapidly advance one's research goals. Also, having spectra, where instrumentation effects have been removed, allows for the computation of standard CIE chromaticity coordinates, which collectively quantify the gamut of all practical colors that may be obtained in fireworks and related pyrotechnics. The authors conducted a series of spectroscopic experiments, isolated the spectra, and produced chromaticity coordinates for some of the most abundant emitters in common pyrotechnic flames.

### Visible Light Flame Spectrometer

The energy source used to produce the spectra was a gas burner of the type typically used in an atomic absorption spectrometer. This type burner was well suited to the needs of a flame spectrometer for this project. Its aspirator provided a ready mechanism to introduce solutions (and fine suspensions) into the flame. The burner produced a fairly narrow, but 4-inch (100-mm) long flame. This provided a long optical path for the spectrometer, thereby increasing its efficiency. The burner and a specially fabricated gas handling system facilitated the use of various and mixed gas sources. At the heart of the system was an Ocean Optics<sup>[5]</sup> CHEM2000 spectrometer installed into a slot in a computer. The spectrometer was connected to a chimney and ambient light shield using a large (400 micron) diameter optical fiber that terminated in an adjustable light-collecting lens. Figure 1 is an illustration of the overall flame spectrometer as configured for this project.

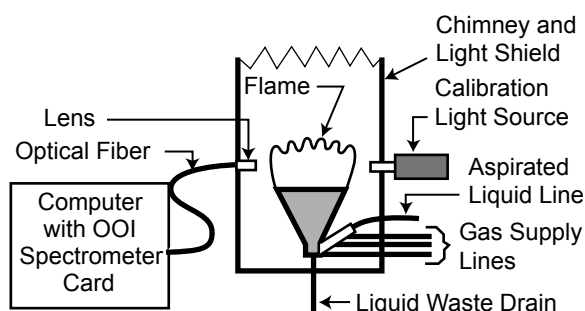


Figure 1. An illustration of the flame spectrometer as configured for this project.

Figure 2 is a diagram of the gas handling system for the spectrometer burner. In producing

the spectra for this project, propane was the only fuel gas used. The supply of air (or air plus oxygen) to the flame was adjusted while aspirating pure water [or a mixture of carbon tetrachloride ( $\text{CCl}_4$ ) and perchloroethylene ( $\text{C}_2\text{Cl}_4$ ) for some of the measurements]. The relative proportion of oxidant supplied was only the amount sufficient to produce clean blue flame tips with a small distinct inner blue cone at the base of the flame. Figure 3 presents the spectrum of the flame and the classic  $\text{C}_2$  (Swan) and CN band groups with perchloroethylene being aspirated into the flame. In each case, it is estimated that the temperature of the flame was approximately 1900 °C. This flame temperature is a little less than that of typical non-metal fueled pyrotechnic flames.<sup>[6]</sup> However, that is not thought to significantly alter the character of the isolated spectra reported in this article.

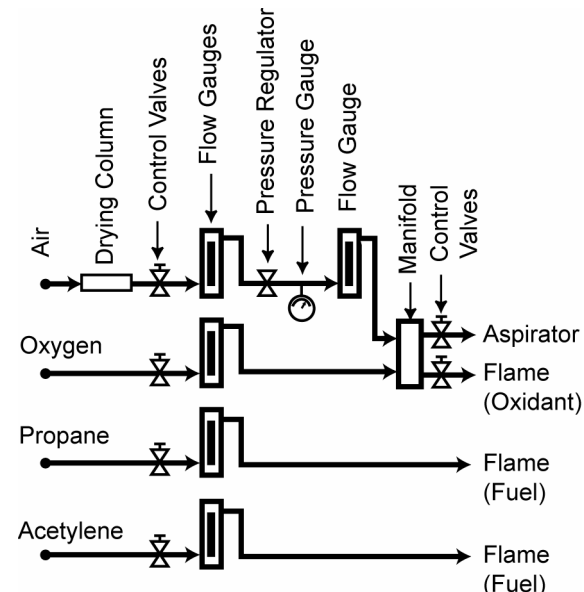


Figure 2. The diagram of the gas handling system for the spectrometer burner.

### Instrument Calibration

The spectrometer was calibrated for wavelength by refining slightly the instrument calibration provided by the manufacturer. This was accomplished by fitting a simple linear equation to the actual and measured wavelengths for 15 sharp and clearly defined atomic peaks of the elements strontium, calcium, barium, potassium, sodium, mercury, and neon. This set of peaks

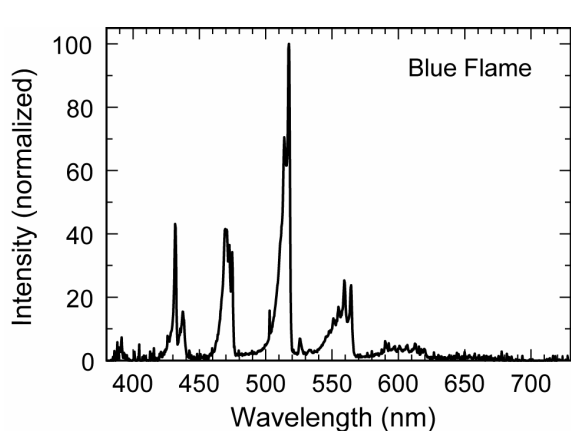


Figure 3. The spectrum of the blue flame with perchloroethylene aspirated into the flame.

ranged from 404.66 to 769.90 nm, which adequately covered the visible light range. (See Figure 4.) The goodness-of-fit parameter,  $r^2$  (where unity is a perfect fit) was greater than 0.9999. The standard error was approximately 0.3 nm, which is less than the spectrometer's measured wavelength interval of approximately 0.4 nm. Note that the resolution of the spectrometer is 1.5 nm full width half maximum (FWHM).<sup>[5]</sup>

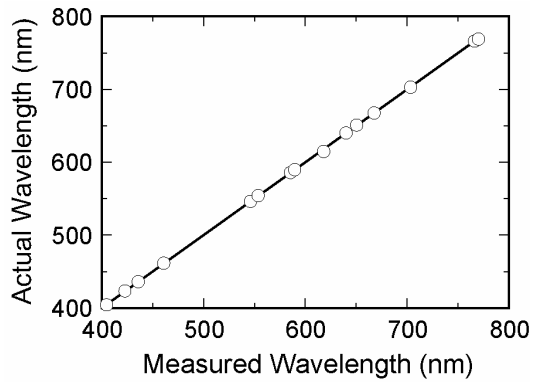


Figure 4. The wavelength calibration curve for the OOI spectrometer.

The optical path that a light ray follows into and through the spectrometer includes the collimating lens, optical fiber, a mirror, and a diffraction grating before it is dispersed onto a linear CCD (charge-coupled device) sensor that converts the light into an instrument-measurable electronic signal. Each of these components attenuates the incoming light by differing degrees at different wavelengths. The CHEM2000 spec-

trometer's diffraction grating exerts the greatest effect. It is designed with a blaze centered on approximately 555 nm<sup>[5]</sup>—the region of the spectrum where it is most efficient.

To calibrate for intensity, the spectrum of the supplied CHEM2000 tungsten-halogen bulb was taken, which is stated by the manufacturer to have a *color* temperature of 3100 K. A software application was developed to calculate the color temperature of tungsten at specified filament temperatures using Planck's Equation, and taking into account the temperature- and wavelength-dependent emissivity of tungsten. It was found that a *filament* temperature of 3035 K produced the closest match of chromaticity coordinates to those calculated for the stated *color* temperature of 3100 K. Both spectra—emissivity and measured—were normalized to unity at 555 nm, corresponding roughly with the blaze of the spectrometer. The corrected spectrum was then divided by the measured spectrum to obtain the required instrument intensity correction factors as a function of wavelength. Figure 5 presents the calibration curve that was required to remove the optical-path effects from the measured spectral data.

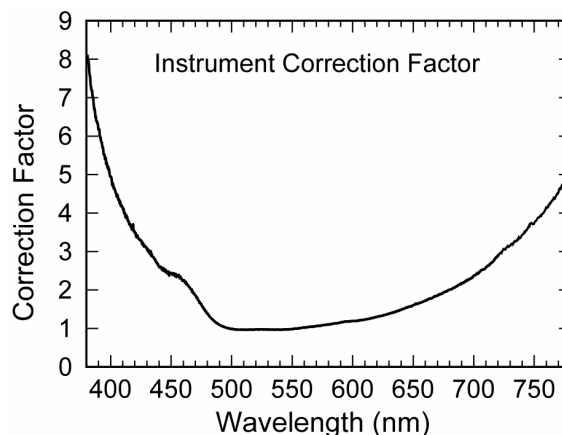
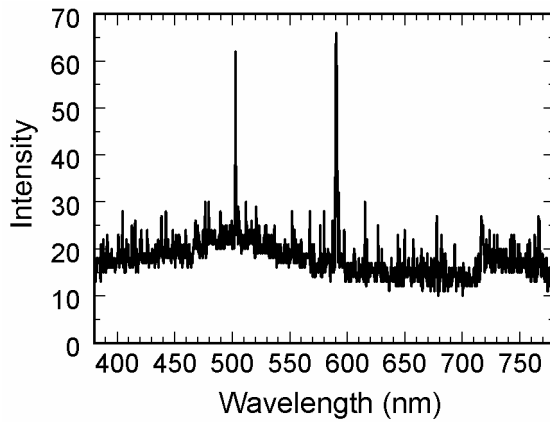


Figure 5. The intensity calibration curve for the OOI CHEM2000 spectrometer.

The CHEM2000 spectrometer is hardware programmable for sample integration time, ranging from as short as a few milliseconds to as long as two seconds per sample. The software acquisition mode used in this project is referred to as “Scope Mode”—a real-time function that is similar to watching an oscilloscope. The output

of this mode is raw spectrometer data, with intensities ranging from 0 to 4095. The CCD and 12-bit analog-to-digital converter both introduce noise into the measurements. It was found that integration times of less than approximately 250 ms resulted in a very good signal-to-noise ratio. For example, the spectrum of the blank (distilled water with no test emitter species present), integrated for 100 ms, accounted for an average intensity reading of 18 parts in 4096, or less than one-half of one percent of the full instrument range. Figure 6 shows the spectrum of a distilled water blank, where the peak at 589 nm is from a trace amount of sodium impurity. The spike at 502 nm is a single channel wide, and there is a lack of any identifiable source. It was concluded that it is probably a slightly noisy CCD detector well. The control software allows for samples to be repeatedly taken and averaged together, to effect additional noise reduction. This feature was utilized whenever the experimental setup permitted its usage.



*Figure 6. Spectrum produced using a blank sample (i.e., distilled water). (Intensity is in "scope units").*

### Sample Preparation

The solutions for the production of the atomic spectra of sodium and potassium, and the molecular spectra of the monohydroxides of strontium, calcium, barium and copper were all prepared in the same way. These simply consisted of a set of fairly dilute aqueous solutions that were made using analytic reagent grade chemicals. The primary criteria used in selecting the chemicals were their availability in the

chemical stocks of the laboratory and for their ability to produce the monohydroxide spectra, while avoiding halides or other species that might produce interferences. The nature of the aqueous solutions and their concentrations are reported in Table 1. These solutions were then aspirated into the propane-air flame of the spectrometer to produce the raw spectral data.

**Table 1. Nature and Concentrations for Aqueous Solutions.**

Chemical Name	Concentration (M)
Sodium hydroxide	0.10
Potassium nitrate	0.10
Strontium nitrate	0.20
Calcium nitrate	0.20
Barium hydroxide	0.10
Copper(II) nitrate	0.20

Samples for the production of the raw spectra for the monochlorides of strontium, calcium, barium and copper as the principal emitters were all made as suspensions. In each case, the appropriate metal chloride was thoroughly dried at 120 °C. While the sample was still hot, it was thoroughly crushed with a preheated mortar and pestle and transferred to a sealed flask for ball milling. The milling was accomplished using steel shot approximately 0.1 inch (2.5 mm) in diameter and using a sufficient amount of carbon tetrachloride ( $\text{CCl}_4$ ) to cover the steel shot. The milling proceeded for 6 to 12 hours during which time the particle size was reduced to an average of approximately 1 micron (as determined using a scanning electron microscope). A magnet was used to remove any trace amount of iron that was worn from the steel shot during milling. To allow for successful aspiration of the suspensions into the spectrometer flame, they were diluted using perchloroethylene ( $\text{C}_2\text{Cl}_4$ ) with a slight addition of the surfactant Neodol 23-5 (an alcohol ethoxylate,  $\text{C}_{22}\text{H}_{46}\text{O}_6$ ). Further, during the time the suspensions were being aspirated into the flame, they were mechanically stirred. To produce a reasonably clean burning flame in the presence of the vaporized carbon tetrachloride and perchloroethylene, and to maintain a flame temperature estimated to be approximately 1900 °C, the propane-air supply was augmented by supplying additional oxygen.

## Data Reduction

After all of the spectra were taken and saved to the computer, they were initially processed to remove instrumentation effects. The method used was the same for all of the gathered spectra, and proceeded in the following order:

- The slight wavelength correction was applied.
- The spectrum was visually inspected:
  - For spectra where there were extensive regions that had no apparent features—flat and near-zero intensity (instrumentation noise only), such as that for potassium and sodium—an average value was taken of the background regions. This average value was then subtracted from the spectrum.
  - For spectra where most of the visible range included features of interest, the removal of the background was more complicated. The intensity values were divided by the integration time of the particular sample, thus converting the intensity from “scope units” into “scope-second units”. A blank with a similar integration time was processed in the same manner, and the resulting spectrum was then subtracted from the spectrum being processed.
- The spectrum was rescaled using the instrument intensity correction factor.
- Any negative intensity values were set to zero.

Having removed instrumentation effects, peak identification and isolation was then performed. While the method varied as to the emitter, it was essentially a peak-by-peak subtraction of the individual species emissions from the composite spectrum, until only the sought-for emitter spectrum remained.

The various reference texts with tabulated wavelengths and emitting species materially helped in the identification of the individual peaks from the various emitting species, as did the few spectrographs found in some of the reference texts. Alkemade and Herrmann's work<sup>[12]</sup> proved valuable in identifying features in the spectra for calcium, barium, and the Swan series of the flame's blue cone. Another text,<sup>[13]</sup> edited

by Mavrodineanu, proved very valuable for identifying copper and copper chloride spectra. Mavrodineanu and Boiteux's work<sup>[14]</sup> was useful for calcium, strontium, and barium. The work of Li et al.<sup>[15]</sup> helped in isolating gaseous barium oxide.

For complex spectra with numerous overlapping peaks of different emitters, the PeakFit software application<sup>[16]</sup> was utilized for peak isolation. Asymmetric peaks were placed at the correct wavelengths that correspond to the tabulated locations of the respective lines and bands for each probable emitter identified in the spectra. The individual peaks were interactively and iteratively adjusted for amplitude and asymmetry until the original spectrum was very closely approximated. In a few cases, an individual peak required a minor shift in wavelength from the tabulated value—on the order of 0.5 to 1.5 nm—to afford the best possible fit. The resulting sets of individual peaks were exported from the peak fitting application to a spreadsheet. The spreadsheet was used to isolate the approximated individual emitters.

Figure 7 illustrates this process: a small region of the measured spectrum of aqueous barium hydroxide is shown. Portions of four fitted peaks [three BaO peaks (centered at 481, 485, and 497 nm) and BaOH centered at 488 nm] and a linear baseline are shown. Figure 8 presents the same portion of the spectrum, where the original spectrum has been plotted along with the fitted

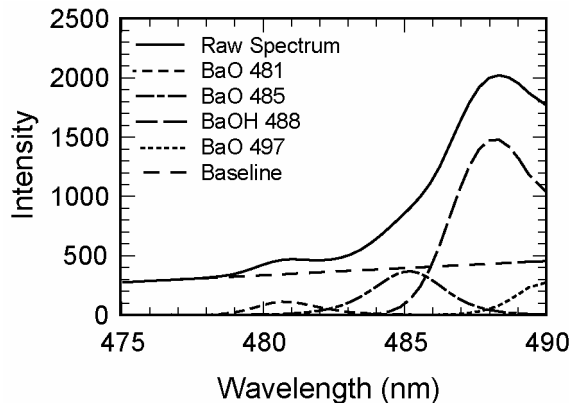
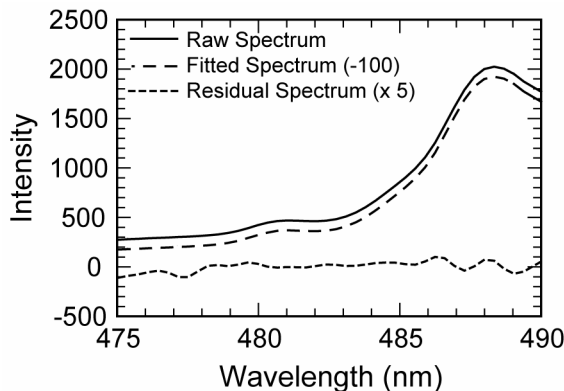


Figure 7. An example of the peak fitting method used to isolate the various contributions to a small portion of the raw barium monohydroxide spectrum.

spectrum (offset by 100 intensity units for clarity). The close approximation of the peak fitting to the original spectrum is evident. Centered about the zero-point of the intensity axis is the residual spectrum, which has been scaled-up by a factor of five to improve its visibility in the graph.



*Figure 8. The result of peak isolation for the same spectral region shown in Figure 7. (Note that the fitted spectrum has been slightly offset from the raw spectrum, and the residual spectrum has been multiplied by 5.)*

After the individual emitter spectra were isolated, a final “cleanup” was made to remove very minor amounts of unwanted, residual noise from the featureless regions of the graphs. This was followed by the calculation of 1931 CIE *xyz* chromaticity coordinates using the standard 2-degree, nanometer-increment, color matching functions.<sup>[17]</sup>

Each of the following spectra has been normalized such that the most intense peak equals 100 intensity units. Thus reported peak intensities can be compared within the same spectrum, but not between different spectra (emitter species).

The composite spectra and those of the various isolated components are presented and discussed below. (Table 2 later in this paper presents the normalized band and line intensities for the various emitting species.) Most of the spectra use a wavelength range of 380–730 nm, which represents the visible light range for most people. There are a few spectra that use the range 380–780 nm to allow inclusion of features in the near infrared. In the discussion of spectral features in the remainder of this text, wavelengths have been rounded to the nearest nanometer.

## Sodium

The raw spectrum of the sodium hydroxide solution (NaOH in H<sub>2</sub>O) had no measurable impurities. It is not shown, because it appeared fundamentally the same as the isolated spectrum of atomic sodium (Na), shown in Figure 9.

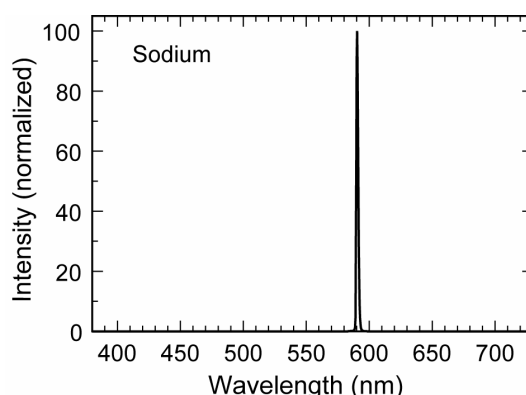


*Figure 9. Spectrum of the isolated atomic sodium doublet peak.*

## Potassium

The spectrum of the potassium nitrate solution (KNO<sub>3</sub> in H<sub>2</sub>O) included a small amount of sodium as an impurity, as is evidenced by the small peak at 589 nm in Figure 10a. (To make it easier to see, the region of the sodium impurity peak was multiplied by a factor of 10.) Also shown in this figure is the very small potassium peak at 404 nm, which has an intensity of 0.058. (To make it possible to see, the region of this peak has been multiplied by a factor of 100.) The sodium peak was removed to produce the pure atomic potassium (K) spectrum in Figure 10b. The peak at 767 nm is about 1700 times more intense than the one at 404 nm. This combination of peaks has a subtle but important effect on the perceived color of potassium flames, as described later. Note that these two graphs use a range of 380–780 nm.

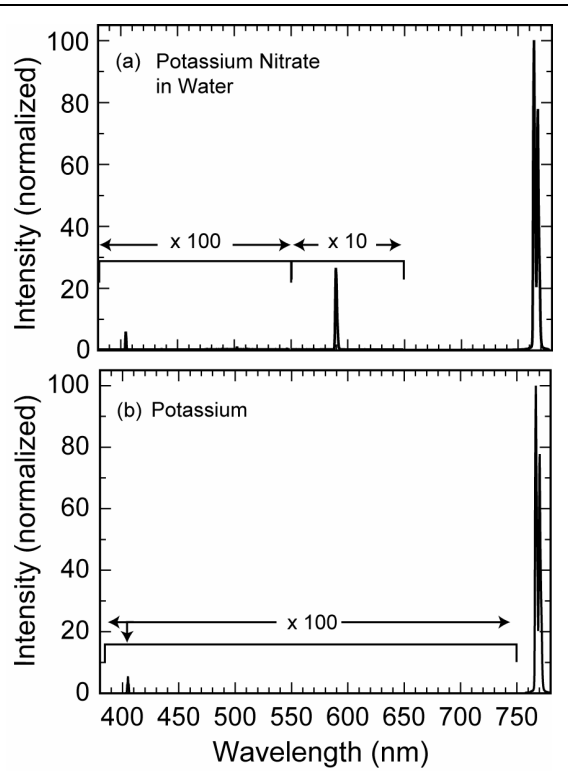
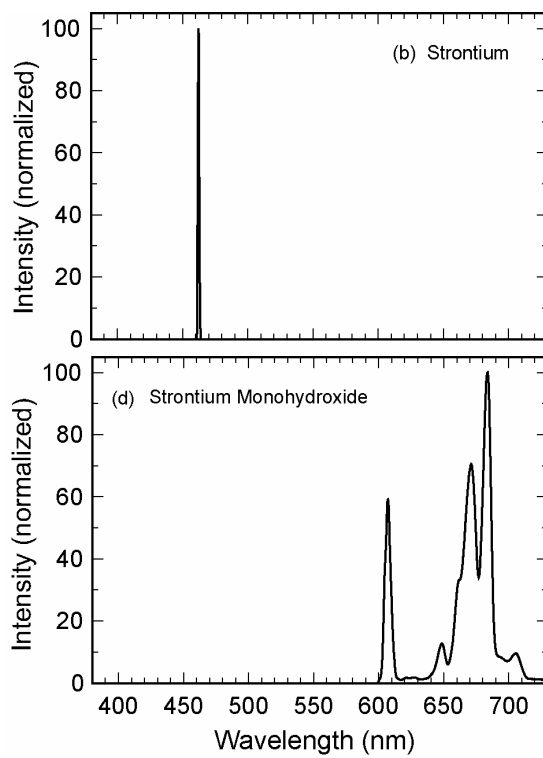
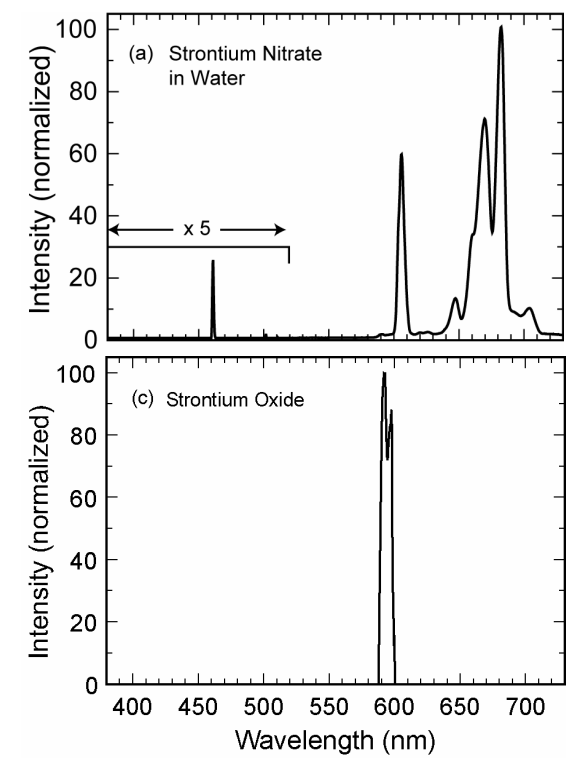


Figure 10. a) The spectrum of potassium nitrate dissolved in water. b) The isolated spectrum of atomic potassium.

## Strontium

The spectrum for the strontium nitrate solution ( $\text{Sr}(\text{NO}_3)_2$  in  $\text{H}_2\text{O}$ ) is presented in Figure 11a. (Note: the region of the atomic strontium peak was multiplied by a factor of 5 to make it easier to see.) After subtracting the minor sodium peak, isolating the individual spectra was straightforward since very few of the observed peaks of atomic strontium (Sr), strontium oxide ( $\text{SrO}$ ), and strontium monohydroxide ( $\text{SrOH}$ ) overlap. The isolated atomic strontium (Sr) peak is shown in Figure 11b. The two main strontium oxide peaks at 595 and 597 nm are barely visible, and the weaker ones—reported to be less than 1/20 the amplitude of the two main peaks—are lost in the intense strontium monohydroxide peaks. For this reason, the graph for strontium oxide (Figure 11c) is necessarily incomplete, but it does provide a useful reference for the two most prominent peaks. The isolated strontium monohydroxide spectrum is presented in Figure 11d.

*Figure 11 [below]. a) The spectrum of strontium nitrate dissolved in water. b) The isolated spectrum of atomic strontium. c) The spectrum of the two strontium oxide peaks that could be cleanly isolated. d) The isolated spectrum of strontium monohydroxide.*



The spectrum for the strontium chloride suspension ( $\text{SrCl}_2$  in  $\text{CCl}_4$ ) is presented in Figure 12a. Subtracted from this spectrum were rescaled atomic strontium, strontium oxide and strontium monohydroxide spectra, resulting in an isolated strontium monochloride ( $\text{SrCl}$ ) spectrum as seen in Figure 12b. It is interesting to note that none of the references in the Table in the appendix mention the two low-intensity peaks centered at about 687 and 700 nm. The character of the peaks—their spacing and width—suggest that they are a continuation of the strontium monochloride spectrum and are included as such.

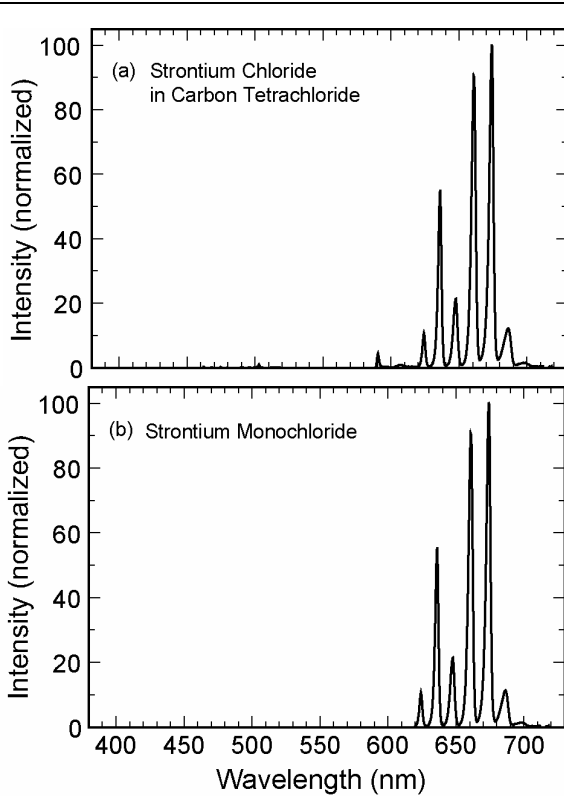


*Figure 12. a) The spectrum of strontium chloride suspended in carbon tetrachloride. b) The isolated spectrum of strontium monochloride.*

## Calcium

The spectrum for the calcium nitrate solution ( $\text{Ca}(\text{NO}_3)_2$  in  $\text{H}_2\text{O}$ ) is presented in Figure 13a. The range for this figure extends from 380 to 780 nm so that the intense atomic potassium peaks, present as an impurity, may be clearly

seen. After subtracting the potassium and sodium peaks, the isolation of the atomic calcium (Ca) peak (see Figure 13b) and the calcium monohydroxide ( $\text{CaOH}$ ) peaks (see Figure 13c), were readily made. Unfortunately, calcium oxide ( $\text{CaO}$ ) was not detected, and it cannot be reported in this work.

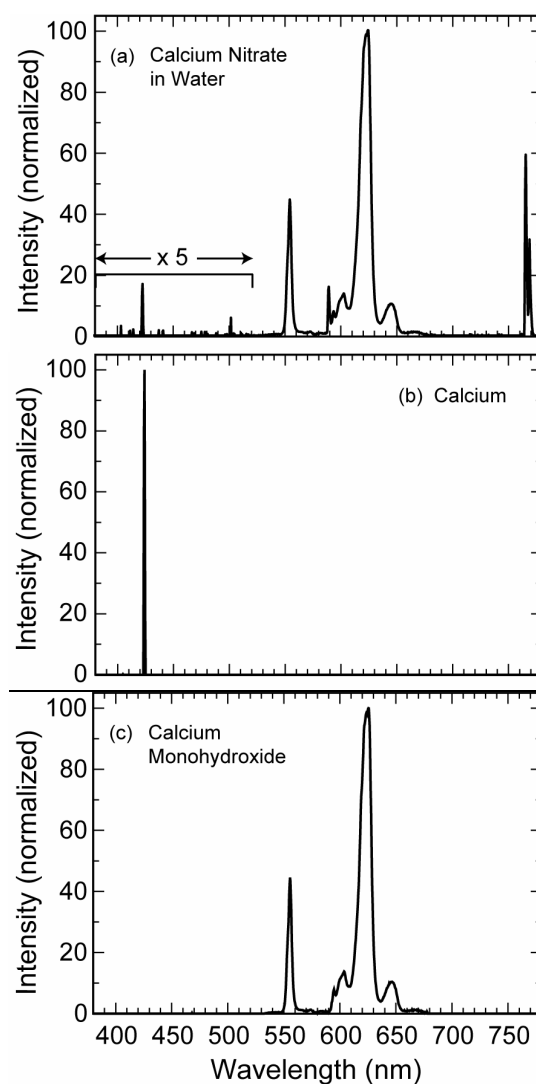


*Figure 13. a) The spectrum of calcium nitrate dissolved in water. b) The isolated spectrum of atomic calcium. c) The isolated spectrum of calcium monohydroxide.*

The spectrum for the calcium chloride suspension ( $\text{CaCl}_2$  in  $\text{C}_2\text{Cl}_4$ ) is presented in Figure 14a. Calcium monohydroxide was rescaled and subtracted from this spectrum, resulting in the isolat-

tion of the calcium monochloride ( $\text{CaCl}$ ) spectrum as seen in Figure 14b.

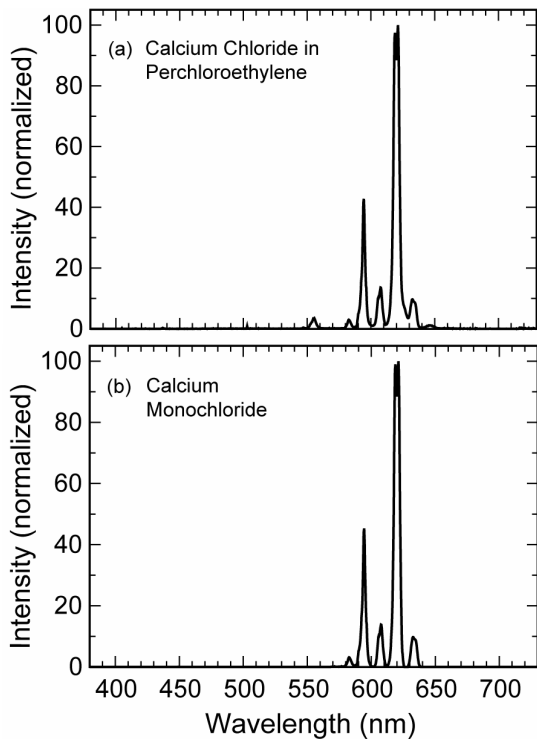


*Figure 14. a) The spectrum of calcium chloride suspended in perchloroethylene. b) The isolated spectrum of calcium monochloride.*

## Barium

The spectrum for the barium hydroxide solution ( $\text{Ba}(\text{OH})_2$  in  $\text{H}_2\text{O}$ ) is presented in Figure 15a. The range for this figure extends from 380 to 780 nm so that the prominent feature centered about 750 nm can be seen. Underlying this complex spectrum is a continuum that is produced by condensed-phase barium oxide ( $\text{BaO}$ ).<sup>[6]</sup> The profile of this continuum (see Figure 15b) was approximated by fitting a curve to the local minima present in the raw spectrum. This continuum was then subtracted from the original spectrum, yielding an intermediate spectrum that represented the gas-phase emitters. Asymmetric peaks were then placed at the wavelengths corresponding to the tabulated locations for atomic barium ( $\text{Ba}$ ), barium oxide ( $\text{BaO}$ ), and barium monohydroxide ( $\text{BaOH}$ ). The approximated barium monohydroxide peaks were thus isolated and are presented in Figure 15c. Likewise, the

peak for atomic barium ( $\text{Ba}$ ) was also isolated and appears in Figure 15d. Finally, the barium monohydroxide and atomic barium peaks were then subtracted from the intermediate spectrum, leaving gaseous barium oxide (see Figure 15e).

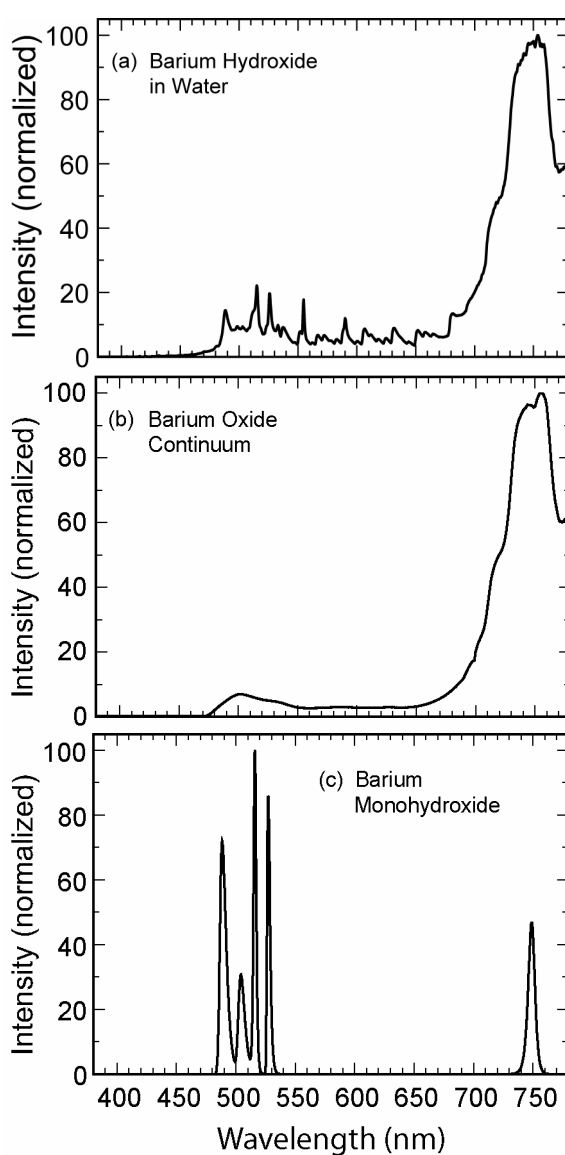


*Figure 15. a) The spectrum of barium hydroxide dissolved in water. b) The spectrum of the condensed phase of barium oxide. c) The isolated spectrum of barium monohydroxide. [continued on next page]*

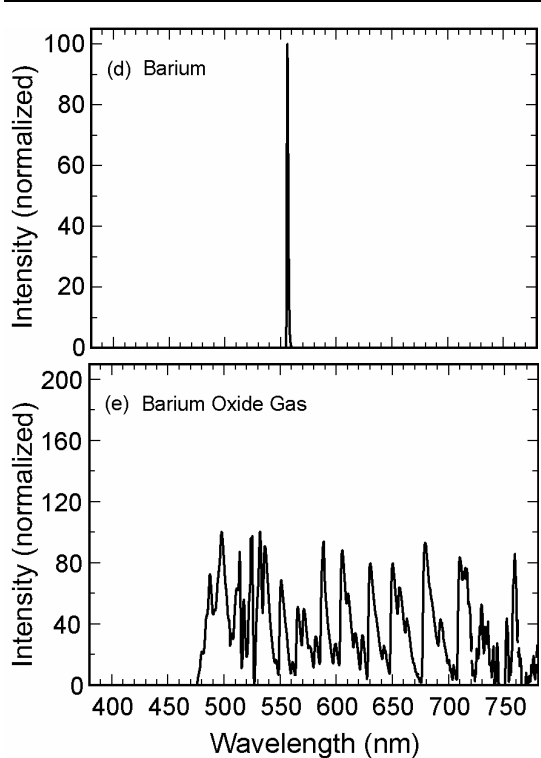


Figure 15. [continued] d) The isolated spectrum of atomic barium. e) The spectrum of vaporized barium oxide.

The spectrum for the barium chloride suspension ( $\text{BaCl}_2$  in  $\text{C}_2\text{Cl}_4$ ) is presented in Figure 16a. The range for this figure extends from 380 to 780 nm so that the peaks for atomic potassium impurities may be seen, as well as the low-intensity barium oxide continuum. Rescaled atomic sodium, potassium and barium, as well as barium oxide and barium monohydroxide spectra were subtracted, leaving an isolated barium monochloride ( $\text{BaCl}$ ) spectrum, as seen in Figure 16b.

## Copper

An attempt was made to acquire copper spectra by using copper nitrate dissolved in water, but the intensity of the peaks was so weak that it required an integration time of 2000 ms. This lead to excessive noise in the spectrum, making it impractical to resolve the individual and complex peaks for atomic copper ( $\text{Cu}$ ), copper hydride ( $\text{CuH}$ ), copper oxide ( $\text{CuO}$ ), and copper monohydroxide ( $\text{CuOH}$ ).

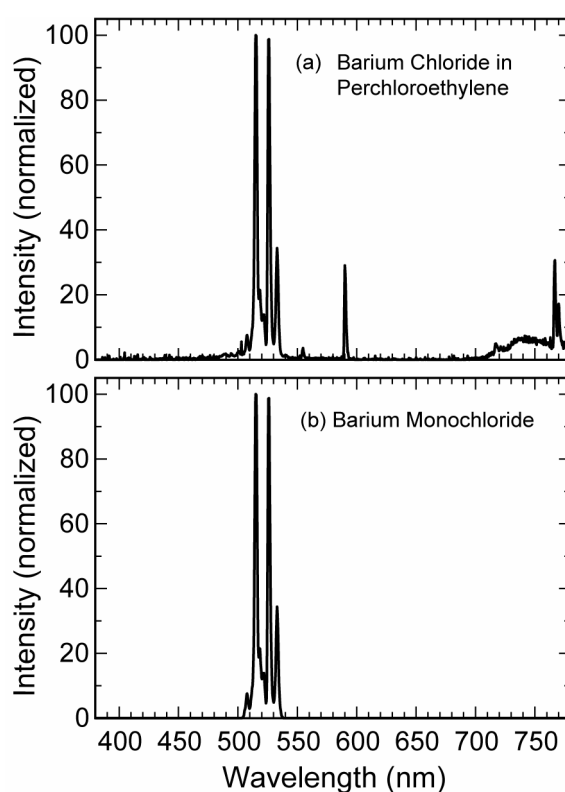


Figure 16. a) The spectrum of barium chloride suspended in perchloroethylene. b) The isolated spectrum of barium monochloride.

Copper(II) chloride in an aqueous solution ( $\text{CuCl}_2$  in  $\text{H}_2\text{O}$ ) was then tried, and this resulted in a reasonably intense and useful spectrum, as seen in Figure 17. Note that this figure is scaled from 380 to 780 nm, clearly showing the atomic potassium peaks, and also the atomic sodium peak at 589 nm that was so intense it was clipped by the spectrometer at the integration time used. This spectrum also includes low-intensity copper monochloride ( $\text{CuCl}$ ) peaks, which further complicated peak identification and isolation. For this reason, a copper chloride suspension in perchloroethylene (discussed later) was processed first so that an isolated copper monochloride spectrum could be obtained, which was then rescaled and subtracted from the aqueous spectrum. This left an intermediate spectrum including peaks for atomic copper, copper oxide, copper monohydroxide, copper hydride, and impurities.

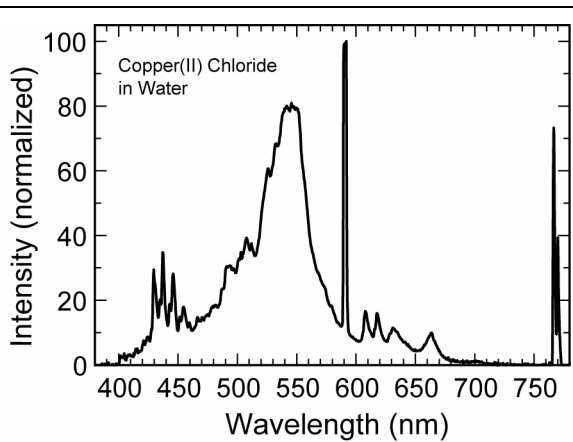


Figure 17. The spectrum of copper(II) chloride dissolved in water.

The copper monohydroxide peaks, located from approximately 490 to 540 nm, are the most prominent features seen in this figure. Copper hydride predominates towards the blue end of the spectrum, even riding up onto the shoulder of the first copper monohydroxide peak. Towards the red end of the spectrum copper oxide predominates, riding on the shoulder of the last copper monohydroxide peak. In a manner similar to that described above for barium hydroxide in water, the peaks for atomic sodium and potassium, copper hydride, copper monohydroxide, and copper oxide were manually placed and shaped using software, and then exported to a spreadsheet.

Interestingly, atomic copper peaks could not be positively identified despite there being a reported 18 peaks in the wavelength range from 380 to 750 nm. It is assumed that conditions were unfavorable for their formation in significant concentrations in the flame.

The atomic sodium and potassium peaks were subtracted from the intermediate spectrum. The individual copper monohydroxide peaks were summed, and this sum subtracted too, thereby eliminating the effect of the pronounced impact of the copper monohydroxide shoulders on copper hydride and copper oxide. The individual peaks for copper hydride and copper oxide were then isolated and cleaned up. Copper hydride and copper oxide are reported to overlap at 445, 446, and 464 nm, but none of these features could be positively discerned. Likewise, the reported (and low intensity) peaks of copper

oxide at 583–584 nm could not be positively identified. Copper hydride and copper oxide spectra are presented in Figures 18a and b. The resulting clean copper hydride and copper oxide spectra were then subtracted from the intermediate spectrum, leaving the copper monohydroxide spectrum, which was then cleaned up and is presented in Figure 18c.

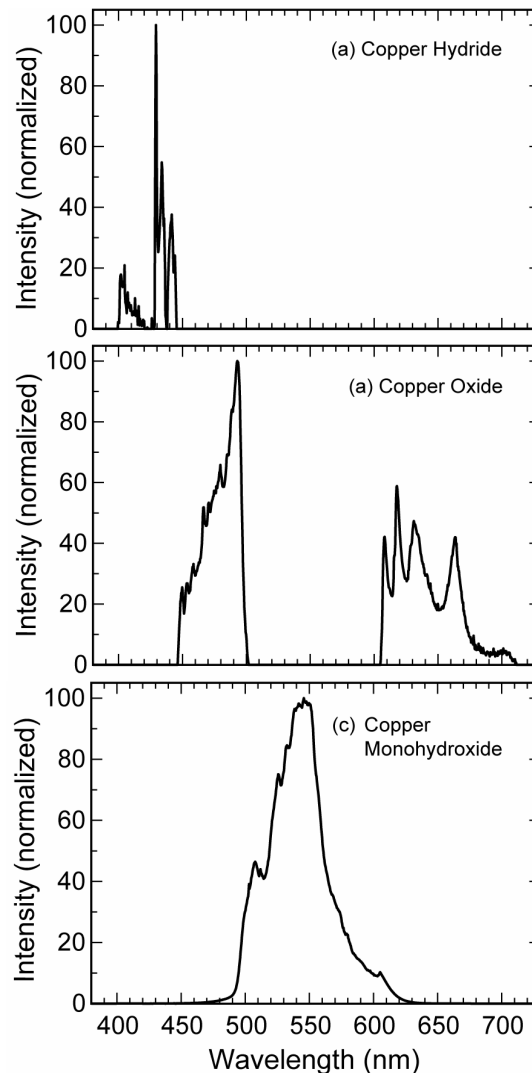


Figure 18. a) The isolated copper hydride spectrum. b) The isolated copper oxide spectrum. c) The isolated copper monohydroxide spectrum.

The spectrum for the copper chloride suspension ( $\text{CuCl}_2$  in  $\text{C}_2\text{Cl}_4$ ) is presented in Figure 19a. Virtually all of the features are associated with copper monochloride, which made isolation of the spectrum straightforward. This was rather fortunate in that it made the isolation of the other copper emitters present in an aqueous-based solution (discussed earlier) much easier. The isolated spectrum for copper monochloride is illustrated in Figure 19b.

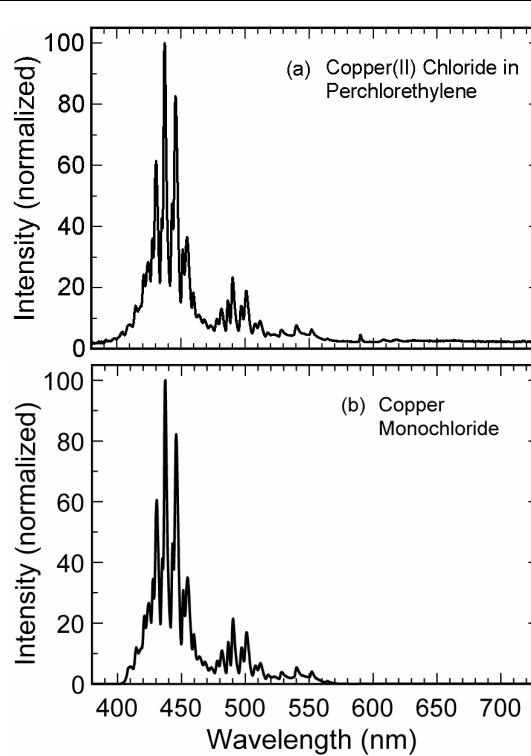


Figure 19. a) The spectrum of copper(II) chloride in perchloroethylene. b) The isolated spectrum of copper monochloride.

## Results

The normalized (to 100 for the most intense peak) line and band intensities for the collection of principal colored flame emitters are presented in Table 2. (A presentation of some of the intensity data collected by others is included as a data table in the Appendix.) Table 3 presents the chromaticity coordinates for the principal emitters investigated in this study.

**Table 2. Normalized Line and Band Intensities for the Principal Color Flame Emitters.**

W. L. <sup>(a)</sup>	R. I. <sup>(b)</sup>	W. L. <sup>(a)</sup>	R. I. <sup>(b)</sup>
<b>SrCl</b>		<b>BaOH</b>	
624	11	488	72
636	55	502	30
648	21	513	100
661	90	524	86
674	100	745	47
687	11	<b>CuCl</b>	
700	1	412	6
<b>SrOH</b>		415	12
606	59	419	12
620	2	421	22
626	2	426	27
649	13	428	35
659	33	431	61
671	70	435	41
682	100	436	100
707	9	443	46
722	1	446	82
<b>CaCl</b>		449	31
581	3	452	35
593	45	460	16
605	11	465	9
608	14	469	7
619	99	476	5
621	100	479	7
633	9	482	11
635	8	485	13
<b>CaOH</b>		489	21
555	45	496	12
572	1	498	17
594	7	509	6
600	11	512	6
604	14	515	3
625	100	526	4
645	10	538	5
665	1	552	4
<b>BaCl</b>		<b>CuOH</b>	
507	8	505	46
514	100	512	44
517	21	524	75
521	14	533	84
524	99	546	100
532	34	605	10

a) W.L. = wavelength.

b) R.I. = relative intensity.

A normalized graph of the luminous sensitivity of the human visual system<sup>[17]</sup> is presented in Figure 20. The wavelength range corresponding to 1% or more of the maximum and extends from approximately 410 to 650 nm, with sensitivity approaching zero beyond this range. The intense potassium peaks at 767 nm (See Figure 10) are at what may be considered the edge of human visual perception and very near the infrared. However, due to its substantial intensity, the peaks at 767 nm produce a measurable shift in the perceived color of any flame that has potassium present in significant amounts. Chromaticity coordinates for the atomic potassium peaks at both 404 and 767 nm, for just the atomic potassium peak at 404 nm, and for just the pair of atomic potassium peaks at 767 nm have been included in Table 3 to demonstrate this effect. The influence of the near-infrared but intense 767 nm peaks is evident.

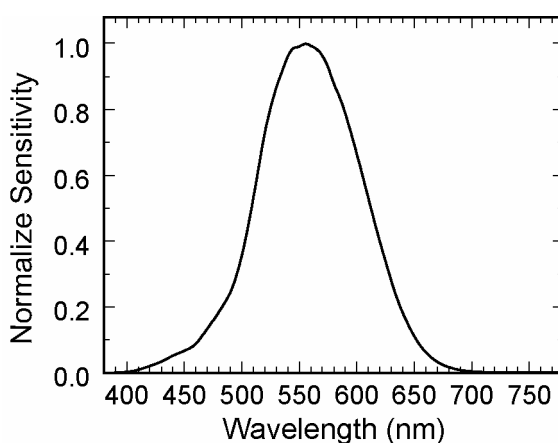


Figure 20. The luminous sensitivity of the human visual system, normalized to 1 at 555 nm.

The solutions produced for this work used reagent grade chemicals; even then the potassium peaks at 767 nm and the ubiquitous atomic

**Table 3. Chromaticity Color Coordinates for the Color Emitters Characterized in this Study.**

Emitter	CIE 1931 Color Coordinates		
	x	y	z
K (with both 404 & 767 nm peaks)	0.676	0.238	0.087
K (404 nm peak only)	0.173	0.005	0.822
K (767 nm peak only)	0.735	0.265	0.000
Na	0.576	0.423	0.001
Ba	0.344	0.653	0.003
BaO (Condensed)	0.380	0.520	0.101
BaO (Gas)	0.406	0.507	0.087
BaOH (approximated)	0.066	0.606	0.328
BaCl	0.094	0.811	0.094
Ca	0.171	0.006	0.824
CaO	NA	NA	NA
CaOH	0.630	0.369	0.001
CaCl	0.661	0.338	0.000
Sr	0.141	0.033	0.826
SrO (Incomplete)	0.593	0.406	0.001
SrOH	0.679	0.321	0.000
SrCl	0.720	0.280	0.000
Cu	NA	NA	NA
CuH	0.167	0.009	0.824
CuO	0.315	0.187	0.499
CuOH	0.290	0.666	0.044
CuCl	0.156	0.073	0.771
Blue Flame (with perchloroethylene)	0.218	0.395	0.387

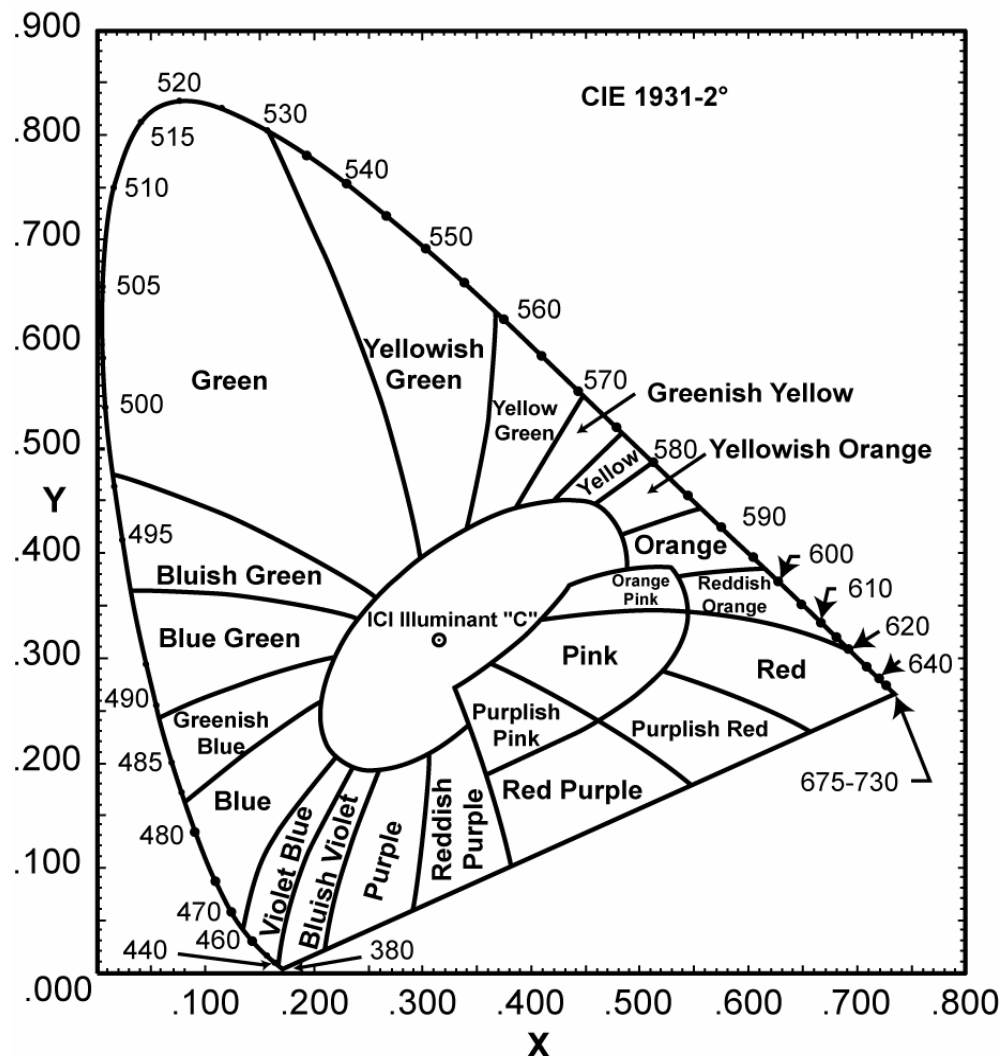


Figure 21. 1931 2° chromaticity diagram.

sodium peak at 589 nm were very often intense. One may conclude that commercial grades of chemicals used in pyrotechnic applications will likely have greater concentrations of impurities such as these, with correspondingly greater interferences and perceived color shifts.

As an aid in interpreting the color point data in Table 3, Figure 21 has been included. This is a black and white rendition of the CIE 1931 2° Chromaticity Diagram. The color points determined in this work are plotted in Figure 22 on simplified versions of the chromaticity diagram of Figure 21. There are two chromaticity diagrams: the first (Figure 22a) displays the location of the color points for the principal colored flame

emitters, and the second (Figure 22b) displays the location of the other color emitters studied.

In Figure 22b, some clarification is needed regarding the identification of some of the color points. The color point for potassium (K) is that including both the 404 and 767 peaks. Only a portion of the strontium oxide spectrum could be isolated from the more intense emitters and thus has not been included in Figure 22b. There are two color points for barium oxide, one corresponding to its emissions when vaporized, designated with the subscript (g), and one for its emissions when condensed, designated with the subscript (cond.).

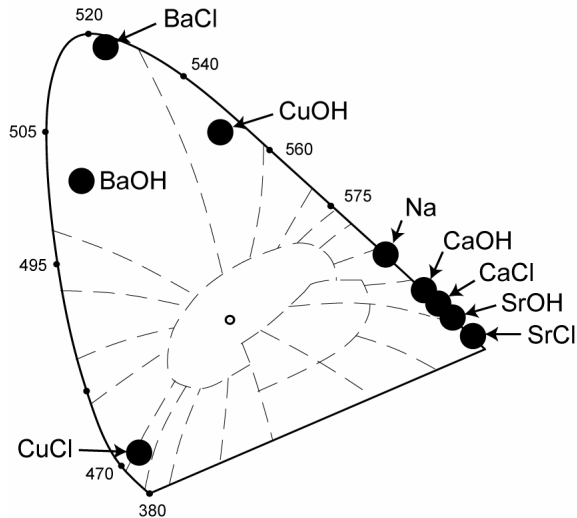


Figure 22a) chromaticity diagram showing the location of the color points for the principal colored flame emitters.

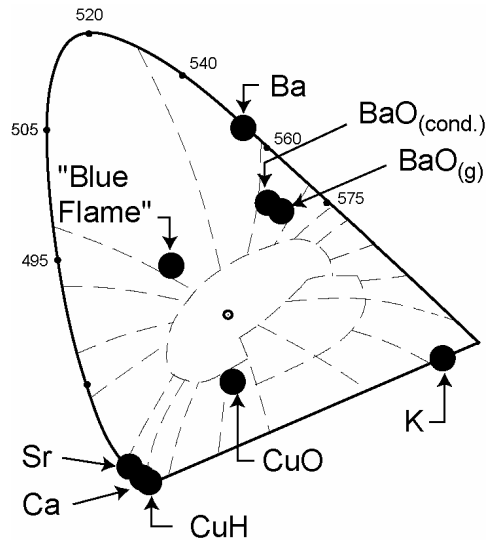


Figure 22b) chromaticity diagram showing the location of the other colored flame emitters studied.

## Conclusions

With more complete and more detailed information regarding the spectral nature of the emitting species in pyrotechnic flames, work to improve flame color should be facilitated. For the most part, this project has been successful in producing that data (with another project anticipated to carry the work further). Upon considering the spectral data for the principal colored flame emitters, it does not appear that progress toward improved flame color will be easy.

Figure 23 summarizes the state of the art with respect to colored flame production, as well as identifying the probable limits of future improvements. The range of colors within the smallest of the quadrangles (shaded) represents the approximate limits of common high quality color formulations.<sup>[18,19]</sup> This covers a relatively small portion of the chromaticity diagram, and much of that consists of what would normally be described as shades of white. It is perhaps fortunate, that observers of fireworks displays do not have light sources producing bright and highly pure color available to them to compare with the colors of the fireworks, many of which would pale by comparison. The small size and central location of this color quadrangle for typical compositions probably also goes a long way toward explaining why photographs and video re-

cords of displays seem to reproduce the colors of the displays so poorly, unless the recorded colors are artificially enhanced.

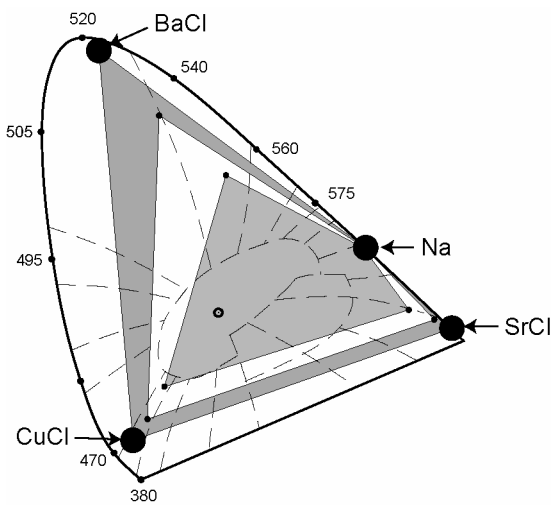


Figure 23. The state of the art for colored flame production. The smallest shaded quadrangle represents the limits of common high quality formulations. The mid-size un-shaded quadrangle demonstrates the very best color formulations reported to date. The largest shaded quadrangle is for the pure color species reported in this paper.

The next larger quadrangle (not shaded) demonstrates the approximate limits of the best color formulations reported to date.<sup>[18,20]</sup> These colors are quite impressive when viewed and are readily discernable as significantly better than even the best of the commonly produced colors. (Unfortunately, there are some limitations associated with the use of these formulations in terms of cost, non-color related performance, and convenience of manufacture.) Using any of the color mixing schemes to produce blended colors,<sup>[21–23]</sup> and even assuming the color formulations are perfectly compatible, one is constrained to produce colors no better than those inside this quadrangle.

Finally there is the outer quadrangle (shaded) formed by the color points of the most desirable color species (the monochlorides of strontium, barium and copper, plus atomic sodium). Unless other, even better color species can be found (and researchers have looked without significant success<sup>[2,24–27]</sup>), this is the ultimate limit of what is possible. In fact, given that flames generally consist of very many chemical species, of which many emit in the visible region, even reaching these limits will probably be impossible to achieve.

### Acknowledgments

The authors gratefully acknowledge the work of all those who have added to the understanding of the chemistry of colored flame, most especially the pioneering work of T. Shimizu and B. Douda. The authors are also grateful to K. Hudson and especially to E.-C. Koch for their comments and suggestions on a draft of this paper.

### References

- 1) T. Shimizu, *Selected Pyrotechnic Publications of Dr. Takeo Shimizu, Part 3, Studies on Fireworks Colored-Flame Compositions*, Journal of Pyrotechnics, 1999.
- 2) B. E. Douda, *Theory of Colored Flame Production*, RDTN No. 71, U.S. Naval Ammunition Depot Crane, IN, USA, 1964.
- 3) B. E. Douda, *Relationships Observed in Colored Flames*, RDTR No. 45, U.S. Naval Ammunition Depot Crane, In, USA, 1964.
- 4) B. E. Douda, "Emission Studies of Selected Pyrotechnic Flames", *J. Optical Soc. America*, Vol. 55, 1965, pp 787–793.
- 5) Ocean Optics, Inc., Dunedin, FL 34698, USA
- 6) T. Shimizu, *Feuerwerk vom physikalischen Standpunkt aus*, Hower Verlag, Hamburg, 1976. Reprinted and translated in four parts by Pyrotechnica Publications (1981 to 1989).
- 7) R. Herrmann and C. T. J. Alkemade, *Chemical Analysis by Flame Photometry*, Translated by Paul T. Gilbert, Interscience Publishers, 1963.
- 8) R. C. Weast, Ed. in Chief, *CRC Handbook of Chemistry and Physics*, 46<sup>th</sup> ed., Chemical Rubber Co., 1965.
- 9) M. L. Parsons and P. M. McElfresh, *Flame Spectroscopy: Atlas of Spectral Lines*, IFI/Plenum, 1971.
- 10) R. W. B. Pearse and A. G. Gaydon, *The Identification of Molecular Spectra*, 3<sup>rd</sup> ed., Chapman and Hall Ltd, 1963.
- 11) A. G. Gaydon, *The Spectroscopy of Flames*, 2<sup>nd</sup> ed., Chapman and Hall, John Wiley & Sons, 1974.
- 12) C. Th. J. Alkemade and R. Herrmann, *Fundamentals of Analytical Flame Spectroscopy*, translated from German by R. Auerbach and Paul T. Gilbert Jr., John Wiley & Sons, New York, 1979.
- 13) R. Mavrodineanu, Ed., Phillips Technical Library, *Analytical Flame Spectroscopy, Selected Topics*, Macmillan, 1970.
- 14) R. Mavrodineanu and H. Boiteux, *Flame Spectroscopy*, John Wiley & Sons, New York, 1965.
- 15) H. Li, C. Focsa, B. Pinchemel, R. J. Le Roy, P. F. Bernath, "Fourier Transform Spectroscopy of BaO: New Ground-State Constants from the  $A^1\Sigma^+ - X^1\Sigma^+$  Chemiluminescence, *Journal of Chemical Physics*, Vol. 113, No. 8, 2000, p 3030.
- 16) PeakFit Version 4.11, Systat, Richmond, CA, USA.

- 17) Color and Vision Research Laboratories, Institute of Ophthalmology, University College, London, and Visual PsychoPhysics, Tübingen Forschungsstelle für Experimentelle Ophthalmologie, University of Tübingen - <http://cvrl.ioo.ucl.ac.uk/cvrl.htm>
- 18) D. E. Chavez, M. A. Hiskey, and D. L. Naud, "High-Nitrogen Fuels for Low-Smoke Pyrotechnics", *Journal of Pyrotechnics*, No. 10, 1999.
- 19) B. V. Ingram, "Color Purity Measurements of Traditional Star Formulas", *Journal of Pyrotechnics*, No. 17, 2003.
- 20) S. Anderson, "Composite Color Stars", *Journal of Pyrotechnics*, No. 8, 1998.
- 21) R. Veline, *A Compatible Star Formula System for Color Mixing*, Self Published, 1989.
- 22) J. H. Baechle, *Pyrocolor Harmony – A Designer's Guide*, Self Published, 1989.
- 23) B. J. and K. L. Kosanke, "Lancework—Pictures in Fire", *Pyrotechnica XV*, 1993; also in *Selected Pyrotechnic Publications of K. L. and B. J. Kosanke, Part 3 (1993 and 1994)*, *Journal of Pyrotechnics*, 1996.
- 24) C. Jennings-White, "Some Esoteric Firework Materials", *Pyrotechnica XIII*, 1990.
- 25) B. T. Sturman, "The Rare Earths as Possible Flame Color Agents", *Journal of Pyrotechnics*, No. 9, 1999.
- 26) E.-C. Koch, "Evaluation of Lithium Compounds as Color Agents for Pyrotechnic Flames", *Journal of Pyrotechnics*, No. 13, 2001.
- 27) E.-C. Koch, "Special Materials in Pyrotechnics Part 2 – Application of Cesium and Rubidium Compounds in Pyrotechnics", *Journal of Pyrotechnics*, No. 15, 2002.

**Appendix — Summary of the Reported Spectral Information for Colored Flame Emitters, Including the Results from this Study [See notes at end of Table.]**

WL (nm)	Intensity							
	A	B	C	D	E	F	G	H
<b>Ba</b>								
552							6	
554	200	170			8.5		10	100
578							9	
602	4							
606	4							
611	12							
645	4							
648	4							
650	50							
653	25							
660	25							
706	4							
<b>BaCl</b>								
507	2				1			8
514	20				10			100
517	4				2			21
521					1			99
524	30				10			34
532	10				3			
<b>BaO</b>								
452	3							
454			vvW					
458	4		vvW					
462	7		vvW					
464	5		vvW					
466	3		vvW					
468	10		vvW		5			
472	5		vvW					
474	10		wM					
478			wM					
479	15							
483	10		wM					
485	50		wM		6			72
487			wM					
490			wM					
494			vvW					
497	30		vvW		3			100

WL (nm)	Intensity							
	A	B	C	D	E	F	G	H
<b>BaO (cont.)</b>								
501	10		vvW					
509	100		W		6			
514								87
521	70		vW		7			
526								97
533								100
535	90	80	vW	4	8	s		90
537			vvW					
540			vvW					
542	5		vvW					
546	20							16
549	70	80	vvW	4	10	vs		
551	10		vvW					68
560	10							
564	40	80	vvW	4	9	vs		
566	5		vvW					
567	10		vvW					51
570	40	80		4	8	s		
571			vvW					
574								36
576	15		vvW					
577			vvW					
581	20		vvW		6	m		
582			vvW					
583			vvW					32
586	40		W	3.5	10	vs		
587		80						
588			W					
589	10		W					93
598	10		vvW		3	w		
604	50	70	W	3.5	9	vs		
608								88
610	20		W		5			
611	10		W					
612			W					59
616	10							
617			vvW		6			34
622			vW		6	m		

WL (nm)	Intensity							
	A	B	C	D	E	F	G	H
<b>BaO (cont.)</b>								
623	15							32
626								29
629	25			W		8	s	
632								79
636				vvW				
642	15			vW				26
649	25			wM		9	vs	
653								71
656	10			vW				57
663				vW				39
666								
670				vvW				
678	50			wM		8	s	
682								56
686	40			vW				33
693	60			vW				26
701				vW				10
710	80			vW		5		50
718				vW				46
725				vW				14
734				vW				32
744				vW				16
752				vW				26
755								
761				vW				41
<b>BaOH</b>								
487				wM				
488	120	100			5			72
497		80			4			
502	30	80			4			30
512				W				
513	140	150			7.5			100
524	80	80			4			86
745	45	50			2.5			47
<b>Ca</b>								
423	10k	250		vS	5			100
428	4							
430	15							
432	3							
444	10							
446	15							
459	8							

WL (nm)	Intensity							
	A	B	C	D	E	F	G	H
<b>CaCl</b>								
383	12							
388	13							
581	250							3
593	500							45
605					2			11
608					2			14
618					10			
619	500				5			99
621	500				10			100
622					5			
633					2			9
635					2			8
<b>CaO</b>								
385			vW					
386			vW					
387					2			
389			vvW					
392			vvW					
397					3			
408					5			
410					4			
413					3			
421					6			
422					5			
424					3			
435					5			
437					5			
438					6			
440					6			
443					3			
451					4			
452					3			
598					8			
600					8			
601					8			
604					3			
606					5			
607					7			
608					5			
609					6			
610					10			
618					6			
626					9			

WL (nm)	Intensity							
	A	B	C	D	E	F	G	H
<b>CaO (cont.)</b>								
628								4
632								2
634								4
636								4
731			vvW					
732			vvW					
733			vvW					
771			vW					
772			vW					6
<b>CaOH</b>								
539			vW					
543	100		W					
546	100							
551	100							
552	200							
553	600							
554	1.2k	500					5	45
555	1k		vS	10	5			
556	400						2	
565	100							
570	100							
572	100	25		0.5				1
578			W					
581	100							
583			W					
594	100							7
597	200							
599	400							
600	400							11
601	600							
602	400	100						
603	400		[a]					
604			M	2				14
605	300							
607	200							
608	200							
609	200							
610	400							
612	200							
622		500		10				
623			vS					
625								100
644		70						

WL (nm)	Intensity							
	A	B	C	D	E	F	G	H
<b>CaOH (cont.)</b>								
645			M	1.4				10
665			W					1
683			vW					
698			vvW					
<b>Cu</b>								
450					4			
455					7			
460					10			
461					8			
465					10			
471					5			
486					4			
487					4			
490					10			
492					8			
497					4			
498					8			
500					7			
511	50		vvW				4	
515							4	
522							5	
570	5							
578	10							
<b>CuCl</b>								
412					5			6
415								12
419	2				6	w		12
421	2				4	w		22
426	5				8	s		27
428	10				7	vs	9	35
433	10				10	vs		35
435	20				9	vs	10	41
436					5			100
441	7				6	s		
443	15				6	vs	9	46
446								82
449	4				4	m		31
452	5				1	m	5	35
460								16
465								9
469								7
476					5	vw	1	5
479					5	vw	2	7

WL (nm)	Intensity							
	A	B	C	D	E	F	G	H
<b>CuCl (cont.)</b>								
482								11
485						8	w	13
488	3					8	w	4
489						6		21
495						4	vw	1
496						5		12
498					4	vw	2	17
509								6
512								6
515					2	m	3	3
526					4	w	6	4
538					2			5
552								4
<b>CuH</b>								
401	5							18
407								12
413								10
416								7
428	30		vvW			vs		100
433	11					m		55
435	10							
436	9							
437	7							
438	9							
439	9							
440	9							
441	9							38
442	7							
443	8							
444	7							24
445	10							
446	11							
465	8							
<b>CuO</b>								
445						8		
446						7		
450								25
452						5		
453						5		27
458						6		33
464						6		
467								52
469						5		

WL (nm)	Intensity							
	A	B	C	D	E	F	G	H
<b>CuO (cont.)</b>								
470					5			
471					7			53
472					7			
477					6			57
480								66
483					4			
485					5			
486					5			69
488					5			83
492					5			100
583					2			
584					3			
605	10				9			
606	50				10			42
615	50				8			
616	50				9			59
628					1			
629					5			
632								47
638					2			
640					5			
643					3			
649					1			
<b>CuOH</b>								
493	60							
505	70	50			5			46
512								44
524	110	70	vvW		7			75
530	110		vvW					
512								84
537	120	100	vvW		10			
533								100
605								10
615-625			vvW					
	[c]	<b>K</b>						
404	500			0.03			5	0.06
405	250	30					4	
580	25							
694	40							
766	40k	10k			10		10	100
770	200k	10k			10		9	78

WL (nm)	Intensity								
	A	B	C	D	E	F	G	H	
	[d]	<b>Na</b>							
568	40								
569	80								
589	800k	30k				10		100	
590	400k					10		9 100	
	[e]	<b>Sr</b>							
461	10k	500				1		10 100	
483								5	
487								2	
496								3	
	<b>SrCl</b>								
389	4								
392	4								
394	4								
396	4								
398	4								
401	4								
624								2 11	
636	20							10 55	
648								4 21	
661	20							10 90	
662								5	
674								5 100	
675	10							5	
676								3	
687								11	
700								1	
	SrO	[f]	[g]	[h]					
390			vvW						
392			vvW						
593									100
595		500	W	1					
597		500		1					88
608	25								
609	20								
610	10								
611	7								
750	5		vvW						
752	7		vvW						
754	10		vvW						
756	10								
787	20								
788	25								

WL (nm)	Intensity							
	A	B	C	D	E	F	G	H
<b>SrOH</b>								
604	3k							
605		5k			10		Str.	
606	7k					vs		59
608							10	
609							6	
610							4	
611							1	
620						vw		2
624	150							
626						vw		2
645		250		0.5				
646	700		M			m		
649								13
659	1.5k	500	W	1		w		13
666	5k	500		1				
671			vs			vs		70
672	4k							
680		250						
682	7k		vs	0.5		vs		100
704	500		wM			m		9
707			W			w		1
722								

### Sources of Spectral Data in Table

- A) R. Herrmann and C. T. J. Alkemade, *Chemical Analysis by Flame Photometry*, Translated by Paul T. Gilbert, Interscience Publishers, 1963. [Note: Does not include peaks with an intensity of one.]
- B) *CRC Handbook of Chemistry and Physics*, 46<sup>th</sup> ed., Robert C. Weast, Ed., Chemical Rubber Co., 1965. [Note: Only air-hydrogen flame values using aqueous solutions reported.]
- C) R. Mavrodineanu and H. Boiteux, *Flame Spectroscopy*, John Wiley & Sons, Inc., 1965 [Note: Only acetylene-air, outer cone values reported.]
- D) M. L. Parsons and P. M. McElfresh, *Flame Spectroscopy: Atlas of Spectral Lines*, IFI/Plenum, 1971. [Note: Only air-hydrogen values reported.]

E) R. W. B. Pearse and A. G. Gaydon, *The Identification of Molecular Spectra*, 3<sup>rd</sup> ed., Chapman and Hall LTD, 1963. [Note: Variety of sources, flame types, furnaces, and arcs reported.] NOTE: Looking at the more recent (4<sup>th</sup>) edition from 1975, there are obviously some deviations between the transitions listed in this Table under E. At the time of writing, the authors did not have this edition available. In all probability – knowing the types of budgets that university libraries face – the older edition may be more readily found.

F) A. G. Gaydon, *The Spectroscopy of Flames* 2<sup>nd</sup> ed., Chapman and Hall, John Wiley & Sons, 1974.

G) B. E. Douda, *Theory of Colored Flame Production*, U.S. Naval Ammunition Depot, RDTN No. 71, 1964. [Note: Values from Gaydon are not reproduced for this column.]

H) This work.

### Table Notes

Note: Some researchers used a non-numerical scale, such as *vvW* for Very Very Weak, *vs* for Very Strong, etc. No attempt was made to convert these to a numerical scale. In addition, there are discrepancies in wavelength assignments between the various sources. No attempt was made to reassign wavelengths.

- a) 604–698 nm designated as “CaOH (?)” in the original text.
- b) Designated as Cu<sub>2</sub>, not Cu, in the original text.
- c) Only values  $\geq 25$  are listed.
- d) Only values  $\geq 25$  are listed.
- e) Only values  $\geq 25$  are listed.
- f) 595 and 597 nm are designated as possibly being Sr<sub>2</sub>O<sub>2</sub> in the original text.
- g) 595 nm is designated as Sr<sub>2</sub>O<sub>2</sub> in the original text.
- h) 595 and 597 nm are designated as Sr<sub>2</sub>O<sub>2</sub> in the original text.